Optical description of solid-state dye-sensitized solar cells. II. Device optical modeling with implications for improving efficiency

ARTICLE *in* JOURNAL OF APPLIED PHYSICS · NOVEMBER 2009

Impact Factor: 2.18 · DOI: 10.1063/1.3204985 · Source: IEEE Xplore

Optical description of solid-state dye-sensitized solar cells: II. Device optical modeling with implications for improving efficiency

David M. Huang,[1] Henry J. Snaith,[2] Michael Grätzel,[3] Klaus Meerholz,[4] and Adam J. Moulé[1,*]

[1]*Chemical Engineering and Materials Science Department, University of California, Davis, CA 95616, USA*

[2]*Clarendon Laboratory, Department of Physics, University of Oxford, Parks Road, Oxford, OX1 3PU, United Kingdom*

[3]*Institut des Sciences et Ingenierie Chimique, École Polytechnique Fédérale de Lausanne, CH-1015 Lausanne, Switzerland*

[4]*Department Chemie, Universität zu Köln, Luxemburgerstrasse 116, 50939 Köln, Germany*

(Dated: May 5, 2009)

We use the optical transfer-matrix method to quantify the spatial distribution of light in solid-state dye-sensitized solar cells (DSCs), employing material optical properties measured experimentally in the accompanying article (Part I) as input into the optical model. By comparing the optical modeling results with experimental photovoltaic action spectra for solid-state DSCs containing either a ruthenium-based dye or an organic indoline-based dye, we show that the internal quantum efficiency (IQE) of the devices for both dyes is around 60% for almost all wavelengths, substantially lower than the almost 100% IQE measured for liquid DSCs, indicating substantial electrical losses in solid-state DSCs that can account for much of the current factor-of-two difference between the efficiencies of liquid and solid-state DSCs. The model calculations also demonstrate significant optical losses due to absorption by spiro-OMeTAD and TiO_2 in the blue and to a lesser extent throughout the visible: as a consequence, the more absorptive organic dye, D149, should outperform the standard ruthenium-complex sensitizer, Z907, for all device thicknesses, underlining the potential benefits of high extinction-coefficient dyes optimized for solid-state DSC operation.

I. INTRODUCTION

Dye-sensitized solar cells (DSCs)[1] provide a cheap and efficient[2] alternative to traditional crystalline silicon solar cells. Standard DSCs use a mesoporous TiO_2 semiconductor matrix covered with a monolayer of a light-absorbing dye and filled with a redox active electrolyte. Despite the relatively high efficiencies of liquid-electrolyte DSCs of more than 11%,[2] concerns over the stability of the electrolyte in long-term applications has led to interest in replacing the redox electrolyte with a solid-state hole conductor. So far, the best performance for a solid-state dye-sensitized solar cell (SDSC) of 5.1%[3] has been obtained with the organic hole conductor 2,2,7,7-tetrakis-(N,N-di-p-methoxyphenyl-amine)-9,9-spiro-bifluorene (spiro-OMeTAD), which is roughly half the record efficiency achieved with a liquid electrolyte. Incomplete filling of the mesoporous TiO_2 matrix by the organic hole conductor[4] limits the optimal device thickness to around 2 μm,[5] which is roughly an order of magnitude thinner than traditional liquid DSCs;[6,7] the use of dyes with higher absorption coefficients has been suggested[5] as a means to compensate for the smaller device thicknesses in SDSCs and thereby improve their efficiency. However, no study to date has quantified the distribution of the optical electric field in SDSCs, which should make it possible to ascribe more accurately the discrepancy between the efficiencies of SDSCs and liquid DSCs to electrical or to optical losses or a combination of the two, thereby indicating ways in which efficiencies could be improved.

In this article, we quantify the spatial distribution of light in SDSCs by using the optical transfer-matrix method.[8] Crucially, we employ, as input into our model, optical properties (namely, the complex refractive indices) of the various layers that make up a SDSC that were accurately measured in the accompanying article (Part I).[9] The article is organized as follows: in Sec. II A, the essential features of the optical transfer-matrix model are presented; in Sec. II B, the experimental procedures by which SDSCs were fabricated and measured is presented; finally, in Sec. III, the optical model is used to calculated the absorption-limited maximum external quantum efficiency, maximum short-circuit current, and spatial light distribution in SDSCs containing either a ruthenium-based dye (termed Z907)[10] or an organic indoline-based dye (termed D149):[6,11] by comparing the model results with the experimental measurements, electrical and optical losses in SDSCs are quantified.

II. METHODS

A. Model

SDSCs consist of multiple thin film layers with different optical properties. In the optical transfer-matrix model[8] used in this work to calculate the distribution of light intensity in SDSCs, the layers are assumed for simplicity to be parallel, smooth, and of uniform thickness. The transfer-matrix method accounts for reflection and transmission at interfaces, absorption within the layers, and optical interference between ingoing and outgoing optical electric fields, which can be significant for the small layer thicknesses (<2 μm) in SDSCs. The transfer-matrix method as applied to solar cells has been

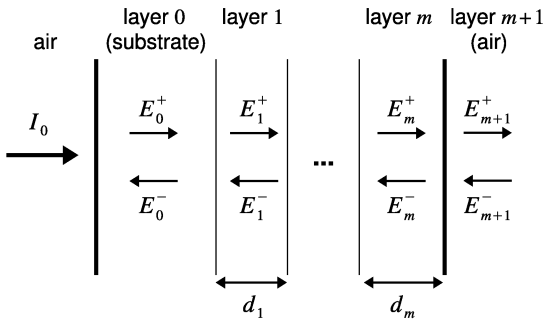

FIG. 1: Schematic of optical model of solar cell comprising m layers of complex index of refraction $\tilde{n}_j \equiv n_j + ik_j$ and thickness d_j, where j denotes the layer number, sandwiched between two layers (0 and $m+1$) of effectively infinite thickness. Light of intensity I_0 arrives at normal incidence from the left of layer 0 (the substrate). $\mathbf{E}_i^+$ and $\mathbf{E}_i^-$ are the optical electric field propagating in the positive (to the right) and negative (to the left) directions, respectively, in layer j.

described in detail elsewhere,[12–16] and so only the essential features of the model will be described here. Figure 1 illustrates schematically the optical model of the solar cell. The only parameters required by the model are the complex index of refraction $\tilde{n}_j(\lambda) \equiv n_j(\lambda) + ik_j(\lambda)$ and thickness d_j, $j = 1, 2, \ldots, m$, of each of the m layers in the solar cell (the glass substrate (layer 0) is assumed to be optically thick). Light of intensity I_0 is assumed to be incident normal to the substrate, the refractive index of air is taken to be 1, and multiple reflections at the air/substrate and substrate/multilayer interfaces are taken into account.[13,14] The transfer-matrix calculation gives the optical electric field $\mathbf{E}_j(x)$ in layer j as a function of distance x to the right of the $(j-1)j$ interface, from which the total absorbed power in layer j at position x can be obtained as[12]

$$Q_j(x) = \frac{2\pi c\epsilon_0}{\lambda} n_j k_j |\mathbf{E}_j(x)|^2 \,, \qquad (1)$$

where c is the speed of light and ϵ_0 is the permittivity of free space. The power dissipated in layer j relative to the incident light intensity is[15]

$$D_j = D_{\rm tot} \left(\int_0^{d_j} Q_j(x) {\rm d}x \right) \Big/ \left(\sum_{i=1}^{m} \int_0^{d_n} Q_i(x) {\rm d}x \right) \,, \quad (2)$$

where $D_{\rm tot} = I_{\rm s}\left(1 - T - R\right)/I_0$[15,16] is the total power dissipated (absorption efficiency) in the m-layer stack (not including the substrate) relative to the incident intensity I_0, $I_{\rm s}$ is the light intensity incident at the substrate/multilayer interface,[16] and T and R are the transmissivity and reflectivity respectively of the multilayer stack (not including the substrate). The dissipation in the SDSCs photo-active layer includes absorption by the TiO_2 matrix, the organic hole conductor spiro-OMeTAD, and the dye. A zeroth-order approximation (which is almost certainly an overestimate) for the light-absorption-limited maximum external quantum efficiency $\mathrm{EQE}_{\rm max}$ is that all light absorbed in the active layer is converted into photocurrent, i.e. $\mathrm{EQE}^0_{\rm max} = D_{\rm AL} \times 100\%$, where $D_{\rm AL}$ is the total dissipation (relative to I_0) in the active layer. To arrive at a more accurate approximation of this upper bound on EQE, we assume that only absorption by the dye can be converted into photocurrent. The complex indices of refraction, $\tilde{n}_{\rm AL}$ and $\tilde{n}_{\rm AL-dye}$ respectively, for the active layer with dye (TiO_2 matrix + dye + spiro-OMeTAD) and without dye (TiO_2 matrix + spiro-OMeTAD) have been measured in the accompanying article (Part I).[9] From Eqs. (1) and (2) $D_j \propto n_j k_j$, and so the proportion of the incident power dissipated in the dye, which is the maximum external quantum efficiency EQEmax in this approximation, can be estimated as

$$\mathrm{EQE}_{\rm max} = \frac{(n_{\rm AL}k_{\rm AL} - n_{\rm AL-dye}k_{\rm AL-dye})}{n_{\rm AL}k_{\rm AL}} \mathrm{EQE}^0_{\rm max}. \quad (3)$$

The internal quantum efficiency can be estimated as $\mathrm{IQE} = \mathrm{EQE}/\mathrm{EQE}_{\rm max}$,[15] where EQE is the experimental external quantum efficiency. The IQE is the efficiency by which photons absorbed by the dye are converted into photocurrent and can therefore be regarded as the electrical efficiency of the device. The maximum possible short-circuit current under one sun was calculated with

$$\mathrm{J}_{\rm sc,max} = e \int_{\lambda_{\rm min}}^{\lambda_{\rm max}} \mathrm{EQE}_{\rm max}(\lambda) b(\lambda) {\rm d}\lambda \,, \qquad (4)$$

where e is the elementary charge and $b(\lambda)$ is the AM1.5 solar photon flux (total irradiance of 1000 $\mathrm{W/m^2}$).[17] The internal quantum efficiency and maximum short-circuit current, IQE^0 and $\mathrm{J}^0_{\rm sc,max}$ respectively, corresponding to $\mathrm{EQE}^0_{\rm max}$ were calculated by analogous methods.

It should be noted in passing that the effect of scattering is neglected in this optical model, but it is not expected to be significant in the SDSCs studied because we are using highly transparent titania pastes; the effect of scattering should be small based on an estimate of the scattering rate scaling as a^3/λ^4,[18] where a is the size of the scattering particles (10-20 nm in the homogeneous titania paste used in the SDSCs studied), which is an order of magnitude smaller than the wavelength λ. Confirming this prediction, the absorption spectra for the active layer filled with or lacking spiro-OMeTAD were found to be essentially identical outside the region in which the spiro-OMeTAD absorbs significantly (<420 nm),[9] whereas the amount of scattering should differ substantially with and without spiro-OMeTAD, due to the reduction in refractive index contrast between the pores and the TiO_2 particles on addition of the organic hole-conductor.

The SDSCs studied with this optical model comprised five layers, in addition to the soda-lime glass substrate: (1) fluorine-doped tin oxide (FTO); (2) compact TiO_2; (3) active layer (TiO_2 + spiro-OMeTAD + dye); (4) spiro-OMeTAD capping layer; and (5) Ag electrode. The complex indices of refraction of the compact TiO_2, mesoporous TiO_2(dyed and bare), spiro-OMeTAD, and Ag

layers were measured experimentally in the accompanying article (Part I).[9] The complex refractive index of specular FTO thin films measured by Rovira and Collins [19] was used for FTO (with values >800 nm obtained by linear extrapolation) and that for BK7 glass at 25°C[20] was used for the glass substrate. DSCs with two different dyes, the organic indoline-based dye D149[6,11,21] and the ruthenium-based dye Z907[10] were studied. Layer thicknesses were chosen to match those of the experimentally measured devices: 400 nm for FTO, 100 nm for compact TiO2, 1.4 μm (Z907) or 2 μm (D149) for the active layer, 200 nm for spiro-OMeTAD, and 200 nm for the Ag electrode.

B. Experimental

Fluorine-doped tin oxide (FTO) coated glass sheets (15 Ω/cm^2, Nipon SG) were etched with zinc powder and HCl (4N) to give the required electrode pattern. The sheets were subsequently cleaned with soap (2% Helmanex in water), distilled water, acetone, ethanol, and finally treated under an oxygen plasma for 10min to remove any organic residues. The FTO sheets were then coated with a compact layer of TiO_2 (100 nm) by aerosol spray pyrolysis deposition at 450°C using oxygen as the carrier gas.[22,23] A home-made TiO_2 nanoparticle paste[24] was doctor bladed onto the compact TiO_2 to give dry film thicknesses between 1.4 and 2 μm, governed by the height of the doctor blade. These sheets were then slowly heated to 500°C (ramped over 30 min) and baked at this temperature for 30 min under an oxygen flow. After cooling, the sheets were cut into slides of the required size and stored in the dark until further use. The final sintered film porosity was 0.6 as determined by nitrogen absorption. Prior to fabrication of each set of devices, the nanoporous films were soaked in a 0.02 M aqueous solution of $TiCl_4$ for 6 h at room temperature in the dark. After rinsing with deionized water and drying in air, the films were baked once more at 500°C for 45 min under oxygen flow with subsequent cooling to 70°C and placed in a dye solution overnight. The ruthenium-based dye used for sensitization was "Z907", an NCS bipyridyl complex with hydrophobic side chains.[10] The organic dye used for sensitization was "D149", an indoline-based push-pull sensitizer with an exceptionally high extinction coefficient of $\sim$68,000 $\mathrm{cm}^{-1}\mathrm{M}^{-1}$.[11] The dye solutions comprised 0.5 mM of Z907 or 0.2 mM of D149 in acetonitrile and *tert*-butyl alcohol (volume ratio 1:1). The hole-transporting material used was spiro-OMeTAD, which was dissolved in chlorobenzene at a typical concentration of 180 mg ml^{-1}. After fully dissolving the spiro-OMeTAD at 100°C for 30 min, the solution was cooled and *tert*-butyl pyridine (tbp) was added directly to the solution with a volume-to-mass ratio of 1:26 μl mg^{-1} tbp:spiro-OMeTAD. Lithium bis(trifluoromethylsulfonyl)imide salt (Li-TFSI) ionic dopant was pre-dissolved in acetonitrile at 170 mg ml^{-1}, then added to the hole-transporter solution at 1:12 μl mg^{-1} of Li-TFSI solution:spiro-OMeTAD. We note that no chemical oxidant was used in the hole-transporter.[25] The dye-coated mesoporous films were briefly rinsed in acetonitrile and dried in air for one minute. A small quantity (20-70 μl) of the spiro-OMeTAD solution was dispensed onto each dye-coated substrate and left for 40 s before spin-coating at 2000 rpm for 25 s in air. The films were then placed in a thermal evaporator, where 150-nm-thick silver electrodes were deposited through a shadow mask under high vacuum (10^{-6} mbar). The device area was defined as the overlap between the FTO anode and gold cathode and was approximately 0.05-0.16 cm^2.

The photovoltaic action spectra were taken using light generated from a halogen lamp monochromated and focused onto the solar cell at an approximate intensity of 0.5 $\mathrm{mW/cm}^2$, calibrated with a calibrated silicon photodiode.

III. RESULTS AND DISCUSSION

A. Maximum external quantum efficiency

The calculated maximum external quantum efficiency $\mathrm{EQE}_{\mathrm{max}}$, experimentally measured external quantum efficiency EQE, and calculated internal quantum efficiency IQE for SDSCs containing the Z907 and the D149 dyes are shown in Fig. 2(a) and (b), respectively. The maximum external quantum efficiency $\mathrm{EQE}^0_{\mathrm{max}}$ and internal quantum efficiency IQE^0 calculated assuming that all light absorbed in the active layer is converted into photocurrent are shown in Fig. 2(c) and (d) respectively for the Z907 and D149 dyes. Figure 2(a) and (b) show that, despite the significant differences between EQE for the two dyes, IQE is approximately 60% in both cases for almost all wavelengths where EQE is measurable. The relative constancy of IQE with wavelength is to be expected, since IQE represents the electrical efficiency and should therefore be independent of optical parameters like the wavelength. Most importantly, this result suggest that the efficiency of SDSCs could be almost doubled if IQE were close to 100%, as it is in standard liquid DSCs.[26] The positions of the oscillations in the experimental curve for EQE for the Z907 dye are reproduced well by the calculated $\mathrm{EQE}_{\mathrm{max}}$; the amplitude of the oscillations in the model curves are more pronounced than those in the experimental curves because the model assumes perfectly flat interfaces between the layers.

If the total amount of light absorbed by the active layer is used to calculate the maximum external quantum efficiency ($\mathrm{EQE}^0_{\mathrm{max}}$), the internal quantum efficiency obtained (IQE^0) shows more variation with wavelength and essentially follows the EQE curve, as shown in Fig. 2(c) and (d). This occurs because $\mathrm{EQE}^0_{\mathrm{max}}$ does not account for optical losses within the spiro-OMeTAD and TiO_2 layers. Comparing $\mathrm{EQE}_{\mathrm{max}}$ with $\mathrm{EQE}^0_{\mathrm{max}}$ or IQE

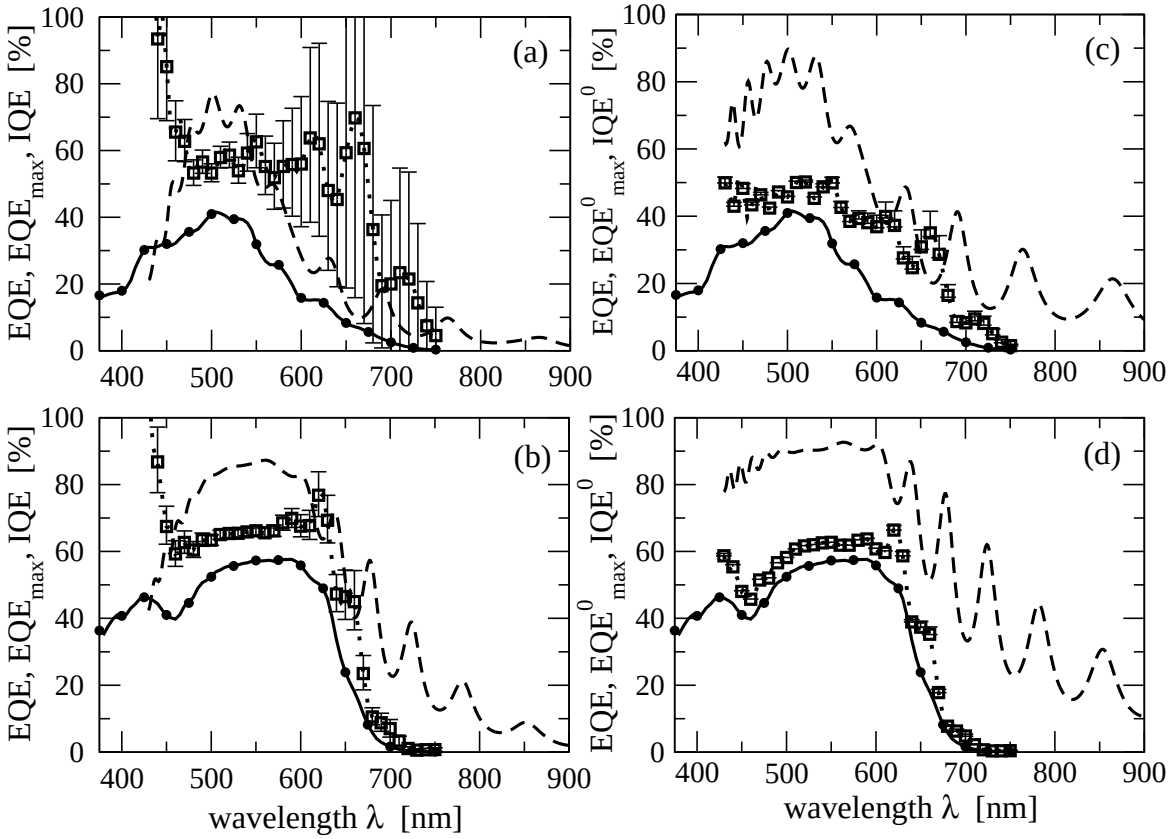

FIG. 2: Maximum external quantum efficiency EQE_{max} from the optical model (dashed lines), external quantum efficiency EQE from experiment (circles + solid lines), and calculated internal quantum efficiency IQE (squares + dotted lines) vs wavelength (solid lines) from the optical model for SDSCs containing the (a) Z907 dye (active layer thickness $d_{AL} = 1.4$ μm) and (b) D149 dye ($d_{AL} = 2.0$ μm). (c) and (d) are the same as (a) and (b), respectively, except that EQE and IQE have been replaced by the maximum external quantum efficiency EQE^0_{max} and internal quantum efficiency IQE^0 calculated assuming all light absorbed in the active layer is converted into photocurrent. The error bars in IQE and EQE were calculated by assuming errors of ± 0.0015 in $k(\lambda)$ for the active layer.

with IQE^0 in Fig. 2(a) and (c) and Fig. 2(b) and (d), it can be seen that a significant proportion of the absorbed light is lost to spiro-OMeTAD or TiO_2, particularly at long wavelengths and for the less absorptive Z907 dye. This is strong evidence that light absorbed in the spiro-OMeTAD or TiO_2 at long wavelengths does not contribute effectively to current generation. At short wavelengths (<450 nm), IQE for both dyes increases to almost 100%, whereas IQE^0 does not show a similar increase. To remind the reader, IQE only accounts for light absorbed in the dye and IQE^0 accounts for light absorbed in the whole active layer. This result suggests that light absorbed by spiro-OMeTAD at these wavelengths, i.e. ground state absorption, is being transferred to the dye, for example by Förster resonant energy transfer (FRET), causing an apparent increased efficiency. However, the relatively low IQE^0 at these wavelengths shows that a substantial proportion of the absorbed light ($\sim$40%) is not being converted into photocurrent.

At wavelengths longer than 680 nm for the Z907 dye and 640 nm for the D149 dye the IQE is significantly reduced compared with the relatively constant value it has over most of the visible spectrum. In our calculation of IQE (from EQEmax using Eq. (3)) we attempt to determine absorption in the dye rather than in the entire active layer. At the longer wavelengths, where the dye absorbance is reduced, the relative difference between the extinction coefficient of the dye, the spiro-OMeTAD/TiO_2 background, and the absolute error in the measurement combine to greatly increase the error in the calculation. Nevertheless, the value of IQE = 60% that is calculated throughout most of the visible spectrum falls outside of the error bars in the low absorbing region. One possible reason for this effect is that the optical properties of spiro-OMeTAD change with aging: preliminary measurements that we have made suggest noticeable changes over time in the absorbance of spiro-OMeTAD at long wavelengths due to oxidation. Because the experimental photovoltaic action spectra and complex refractive indices in the optical model were measured at different times after layer deposition (soon after vs weeks later), the modeled optical characteristics

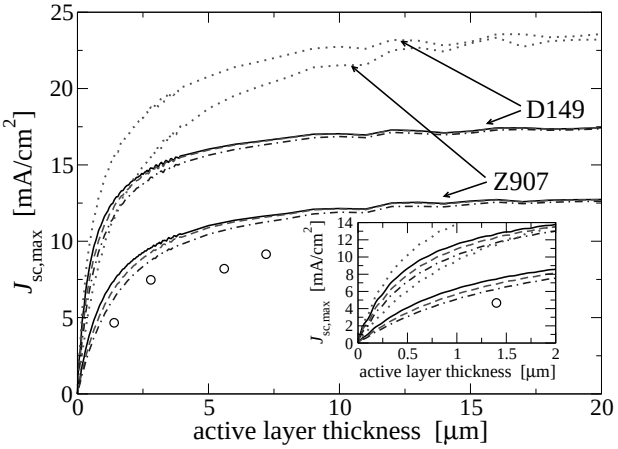

FIG. 3: Maximum short-circuit current density $J_{sc,max}$ vs active layer thickness for SDSCs containing the Z907 dye (lower set of curves) and D149 dye (higher set of curves) with different metal electrodes (solid lines: Ag (200 nm); dashed lines: Au (200 nm); dot-dashed lines: Au (30 nm). Also shown (dotted line) is the maximum short-circuit current density $J^0_{sc,max}$ calculated by assuming all light absorbed by the active layer can be converted into photocurrent (for a 200-nm Ag electrode). The experimentally measured IPCE spectrum integrated over the AM1.5 solar spectrum for SDSCs incorporating K68 (circles), a similar sensitizer to Z907, taken from Ref.[29] are also shown. Inset: A close-up of the small thickness region for the curves in the main figure.

at long wavelengths could differ from those of the fabricated devices. Another explanation for the reduced IQE between 650 and 800 nm is that the excited dye perhaps does not effectively transfer electrons to the TiO_2 near the absorption edge. There have been observations of "hot" electron transfer in dye-sensitized systems[27,28] and this could lead to a reduction in injection efficiency near the band edge if the excited state of the dye is close to or higher in energy than the TiO_2 conduction band. Without in-depth spectroscopic investigation, however, we can speculate no further on these points and, due to the significant measurement error in this low absorbing region, do not wish to draw solid conclusions here. We are, however, investigating this further.

B. Maximum short-circuit current density

The maximum short-circuit current density $J_{sc,max}$ calculated by using Eq. (4), which assumes that only light absorbed in the dye contributes to photocurrent, is plotted in Fig. 3 as a function of the active layer thickness. Also shown in Fig. 3 is the maximum short-circuit current density $J^0_{sc,max}$ calculated assuming that all light absorbed in the active layer is converted into photocurrent. If all light absorbed by the dye, TiO_2, and spiro-OMeTAD in the active layer is assumed to be converted into photocurrent, the maximum short-circuit current density ($J^0_{sc,max}$) for both dyes approach the same value for large active layer thicknesses because essentially all of the light that is not reflected from the front of the device is absorbed by the active layer. However, if only light absorbed by the dye is assumed to contribute to photocurrent, the current density ($J_{sc,max}$) is significantly lower, demonstrating that substantial losses occur in the SDSCs due to competitive absorption by spiro-OMeTAD and TiO_2. The losses are more severe at all device thicknesses up to 20 μm for the less absorbing sensitizer, Z907, with the differences between the organic D149 dye and the Z907 ruthenium complex being most signficat for thinner devices. Currently, the film thickness of a practical device is limited to around 2 μm due to problems with pore filling.[29] For thin films it is apparent that a higher extinction coefficient dye should be advantageous. Furthermore, our findings imply that regardless of film thickness, higher extinction-coefficient dyes are advantageous, since the light harvesting in the sensitizer competes with absorption in the rest of the medium. We note though that the observed differences here probably overestimate the true losses since our results do not take into account possible charge generation or energy transfer from the TiO_2 or spiro-OMeTAD. It should also be noted that the range of active layer thicknesses studied here far exceeds those achievable for SDSCs due to inadequate pore filling by the organic hole conductor for devices thicker than 2 μm.[4,9,29]

Experimental data for the short-circuit current density as a function of active layer thickness for comparison with the calculated results in Fig. 3 does not currently exist for SDSCs containing the D149 or Z907 dye. But such data is available for SDSCs containing K68, a sensitizer that is spectroscopically almost identical to Z907. Figure 3 shows the experimentally measured IPCE spectrum integrated over the AM1.5 solar spectrum for solid-state DSCs of varying thickness incorporating K68.[29] The experimental points for K68 are all approximately 63 to 77% of the calculated $J_{sc,max}$ for Z909 at the same thicknesses, comparable with the value of IQE $\approx$ 60% that would be expected if IQE were constant across the spectrum, as our optical modeling results indicate to be approximately true. The agreement is not perfect, partly because IQE is not completely constant over the spectrum, increasing sharply for $\lambda < 450$ nm due to charge generation or energy transfer from TiO_2 or spiro-OMeTAD, as discussed earlier. In addition, despite the spectroscopic similarity of Z907 and K68, there is some evidence that electrical losses are slightly lower for K68, which was found to give the lowest charge recombination and highest efficiency SDSCs among a series of dyes similar to Z907.[3] Our results suggest that electrical losses of around 25% or more occur even in SDSCs using the efficient K68 dye, once again reinforcing our point that improving electical efficiency in SDSCs, and not just light absorption, is crucial to achieving power efficiencies comparable to those of liquid DSCs.

Figure 3 also shows that, for small active layer thicknesses around those for typical SDSCs ($d_{AL} \approx 2$ μm),

significant losses (>10% for Z907) occur when a 30-nm Au electrode is used instead of a 200-nm Ag electrode. Experimental measurements of SDSCs similar to those modeled in this work, except for the use of the K68 dye, have shown comparable losses of around 20% for a 30-nm Au electrode vs a 200-nm Ag electrode,[3]. Increasing the thickness of the Au electrode from 30 nm to 200 nm reduces the losses (to about 5% for Z907 for $d_{\mathrm{AL}} \approx 2$ μm), but the higher reflectivity of Ag compared with Au makes Ag a better choice for a given electrode thickness. These results indicate that, for experimentally used metal electrode thicknesses, there are small but significant optical losses due to transmission of light through the entire SDSC. Such losses should be insignificant for standard electrochemical DSCs due to the much larger active layer thicknesses used in these devices.

C. Spatial light distribution

The behavior of the calculated maximum short-circuit current density in Fig. 3 and maximum external quantum efficiency in Fig. 2 is more clearly understood by examining the calculated distribution of light intensity inside a SDSC. Figure 4 shows the spatial light distribution for SDSCs containing (a) no dye and containing the D149 dye for (b) 530-nm and (c) 640-nm light. Similar behavior to Fig. 4(b) and (c) is observed for the Z907 dye, although with less attenuation of the light intensity near the absorption maximum, due to the lower absorption coefficient of the Z907 dye.

Figure 4(a) illustrates the reason for the significant difference between $J_{sc,max}$ and $J^0_{sc,max}$ in Fig. 3, namely the strong absorption by spiro-OMeTAD (and, to a lesser extent, TiO_2) at wavelengths relatively close to the absorption maximum of the dye: almost no light at 380 nm is transmitted more than a few hundred nm through a device containing only spiro-OMeTAD and TiO2 and no dye. Although the absorption maxima of the D149 and Z907 dyes are at higher wavelengths than this value, these dyes do absorb substantially near 380 nm: strong absorption by spiro-OMeTAD at this wavelength could therefore lead to significant efficiency losses. The more absorptive D149 dye competes more effectively with spiro-OMeTAD for light than the Z907 dye, resulting in the higher $J_{sc,max}$ for D149 than for Z907 shown in Fig. 3.

Figure 4(b) shows, as expected, that for light with a wavelength near the absorption maximum of the D149 dye around 530 nm, the distribution of light is non-uniform, with the highest light intensity close to the front of the device. This results shows that, at least for wavelengths where the dye absorbs strongly, it is not absorption losses due to the thinness of SDSCs compared with liquid DSCs that limit efficiency. Rather, as discussed above, it is substantial electrical losses of roughly 40% across the visible spectrum that largely explain the differing efficiencies of solid-state and liquid DSCs. Absorption losses do occur at long wavelengths far from the absorption maximum, as shown in Fig. 4(c) for 640-nm light, in which, aside from periodic oscillations in the light intensity, the distribution of the light intensity is uniform across the active layer, indicating that much of the incident light is reflected from the metal electrode and from the device as a whole.

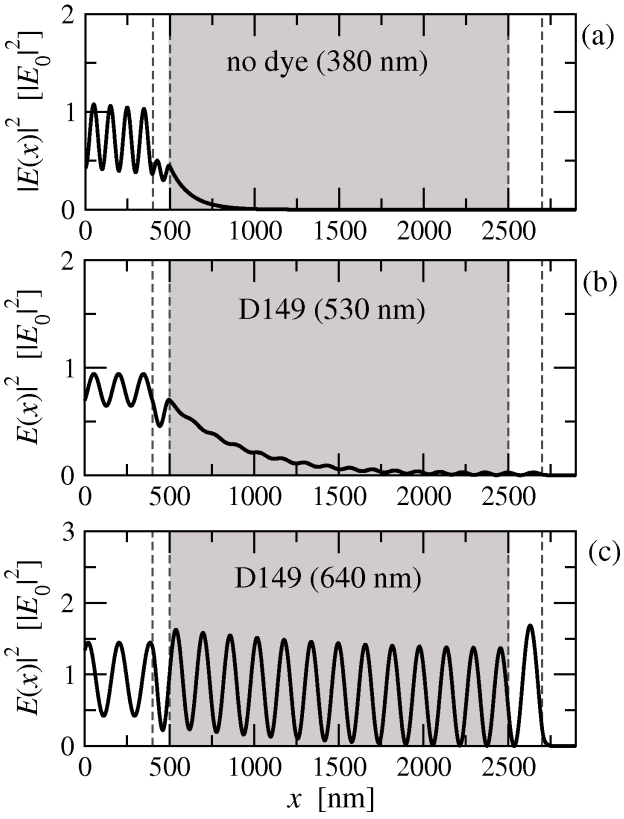

FIG. 4: Square of magnitude of calculated optical electrical field, $|E(x)|^2$, as a function of the distance x from the substrate/multilayer interface (in units of the squared magnitude of the electric field incident on the glass substrate, $E_0^2 2 \propto I_0$) in a SDSC (a) containing no dye for a wavelength of $\lambda = 380$ nm and containing the D149 dye for (b) $\lambda = 530$ nm and (c) $\lambda = 640$ nm. The dashed vertical lines demarcate the boundaries between (from left to right) the FTO (400 nm), TiO_2 compact (100 nm), active (2 μm), spiro-OMeTAD (200 nm), and Ag electrode (200 nm) layers. The active layer is also shaded in gray.

Given the incomplete filling of pores near the front of the device by the organic hole conductor in SDSCs,[4,9,29] the strong absorption near the absorption maximum of the dye in this region of the device would suggest a potential electrical loss mechanism in SDSCs, since a large proportion of excitons would be generated in a region where hole mobility would be reduced. However, it can be seen that the calculated IQE in Fig. 2 for D149 and Z907 is essentially constant with wavelength, indicating that recombination losses do not depend on the light intensity at the front of the device for devices of the thickness studied in this work ($\sim$2 μm). Pore filling could

pose a problem for thicker devices, and this is an issue that needs to be investigated further.

IV. CONCLUSIONS

In summary, we have used the optical transfer-matrix method and accurately measured optical properties of the various layers in a solid-state dye-sensitized solar cell (SDSC) to determine the spatial distribution of light in these solar cells and calculate the maximum external quantum efficiency and short-circuit current of SDSCs for different wavelengths and layer thicknesses. By these means, we have been able to distinguish between electrical and optical losses in these devices. Comparisons with experimental measurements of SDSCs containing either a ruthenium complex termed Z907 or an organic dye termed D149 show that the internal quantum efficiency of both these devices is around 60% across the wavelength spectrum, regardless of the dye, indicating significant electrical losses that are not present in standard liquid DSCs, for which the IQE is close to 100%.[26] This result suggests that, although improving light absorption by the dye in SDSCs is an important goal, substantial improvements may be achieved by optimizing electrical characteristics such as charge transfer, separation, and transport: eliminating these electrical losses could almost double the efficiency of SDSCs. Our calculations also indicate that there are significant optical losses due to absorption by the spiro-OMeTAD and TiO_2. The more absorptive D149 dye is shown to perform significantly better than the Z907 dye for all device thicknesses.

Acknowledgments

This project was supported by the United States Department of Energy under Award Number DE-FG36-08GO18018 and by EPSRC.

* Electronic address: amoule@ucdavis.edu

1. B. O'Regan and M. Grätzel, Nature **353**, 737 (1991).
2. M. Grätzel, Chem. Lett. **34**, 8 (2005).
3. H. J. Snaith, A. J. Moulé, C. Klein, K. Meerholz, R. H. Friend, and M. Grätzel, Nano Lett. **7**, 3372 (2007).
4. L. Schmidt-Mende and M. Grätzel, Thin Solid Films **500**, 296 (2006).
5. L. Schmidt-Mende, S. M. Zakeeruddin, and M. Grätzel, Appl. Phys. Lett. **86**, 013504 (2005).
6. S. Ito, S. M. Zakeeruddin, R. Humphry-Baker, P. Liska, R. Charvet, P. Comte, M. K. Nazeeruddin, P. Péchy, M. Takata, H. Miura, et al., Adv. Mater. **18**, 1202 (2006).
7. A. Hagfeldt and M. Grätzel, Acc. Chem. Res. **33**, 269 (2000).
8. O. Heavens, *Optical Properties of Thin Solid Film* (Dover, New York, 1991).
9. A. J. Moulé, D. M. Huang, H. J. Snaith, M. Kaiser, G. M., and K. Meerholz (2009), in preparation (Part I of this article).
10. P. Wang, S. M. Zakeeruddin, J. E. Moser, M. K. Nazeeruddin, T. Sekiguchi, and M. Grätzel, Nat. Mater. **2**, 402 (2003).
11. T. Horiuchi, H. Miura, K. Sumioka, and S. Uchida, J. Am. Chem. Soc. **126**, 12218 (2004).
12. L. A. A. Pettersson, T. Johansson, F. Carlsson, H. Arwin, and O. Inganas, Synth. Met. **101**, 198 (1999).
13. P. Peumans, A. Yakimov, and S. R. Forrest, J. Appl. Phys. **93**, 3693 (2003).
14. P. Peumans, A. Yakimov, and S. R. Forrest, J. Appl. Phys. **95**, 2938 (2004).
15. A. J. Moulé and K. Meerholz, Appl. Phys. B **86**, 771 (2007).
16. D. W. Sievers, V. Shrotriya, and Y. Yang, J. Appl. Phys. **100** (2006).
17. The lower integration limit, $\lambda_{\min}$, in Eq. (4) was taken to be 430 nm, which was the lowest wavelength at which reliable values for $\tilde{n}$ could be obtained for the active layer.[9] It can be estimated from the experimental data presented in this work that wavelengths less than 430 nm contribute less than 0.6 mA/cm^2 to the short-circuit current J_{sc}. The upper integration limit, $\lambda_{\max}$, was taken to be 830 nm, which is roughly to the upper wavelength limit of photocurrent generation in liquid DSCs for the dye sensitizers studied in this work.[6,10] Although the calculated EQE_{max} extends beyond 830 nm, this result is largely due to the large errors in the small measured extinction coefficient at long wavelengths (the error bars in EQE_{max} above 800 nm for both dyes encompass $EQE_{max} = 0$), and so the EQE_{max} above this wavelength can justifiably be ignored in calculating $J_{sc,max}$.
18. A. Usami and H. Ozaki, J. Phys. Chem. B **109**, 2591 (2005).
19. P. I. Rovira and R. W. Collins, J. Appl. Phys. **85**, 2015 (1999).
20. Luxpop (thin film and bulk index of refraction and photonics calculations): http://www.luxpop.com.
21. H. Snaith, A. Petroza, S. Ito, H. Miura, and M. Grätzel, Adv. Funct. Mater. (2009), in press.
22. L. Kavan and M. Grätzel, Electrochim. Acta **40**, 643 (1995).
23. H. J. Snaith and M. Grätzel, Adv. Mater. **18**, 1910 (2006).
24. C. J. Barbe, F. Arendse, P. Comte, M. Jirousek, F. Lenzmann, V. Shklover, and M. Grätzel, J. Am. Ceram. Soc. **80**, 3157 (1997).
25. H. J. Snaith and M. Grätzel, Appl. Phys. Lett. **89**, 262114 (2006).
26. M. K. Nazeeruddin, P. Péchy, and M. Grätzel, Chem. Commun. **18**, 1705 (1997).
27. B. Wenger, M. Grätzel, and J. E. Moser, J. Am. Chem. Soc. **127**, 12150 (2005).
28. R. Huber, J. E. Moser, M. Grätzel, and J. Wachtveitl, J. Phys. Chem. B **106**, 6494 (2002).
29. H. J. Snaith, R. Humphry-Baker, P. Chen, I. Cesar, S. M. Zakeeruddin, and M. Grätzel, Nanotechnology **19** (2008).